

# On the Methods of Determining the Radio Emission Geometry from Pulsar Magnetospheres

J. Dyks<sup>1</sup>

*Laboratory for High Energy Astrophysics, NASA/GSFC, Greenbelt, MD 20771, USA*

B. Rudak

*Nicolaus Copernicus Astronomical Center, 87-100 Toruń, Poland*

and

Alice K. Harding

*Laboratory for High Energy Astrophysics, NASA/GSFC, Greenbelt, MD 20771, USA*

## ABSTRACT

We correct the relativistic phase shift method of determining the radio emission geometry from pulsar magnetospheres proposed by Gangadhara & Gupta (2001). The correction provides a method of determining radio emission altitudes which does not depend on the viewing geometry and does not require polarization measurements. We propose to apply the method to the outer edges of averaged radio pulse profiles to identify magnetic field lines associated with the edges of the pulse and, thereby, to test the geometric method based on the measurement of the pulse width at the lowest intensity level. Another relativistic method proposed by Blaskiewicz et al. (1991) is not accurate enough to serve as the test. We provide comprehensive discussion of the shortcomings of the relativistic methods. Moreover, we show that estimates of rotational distortions of the vacuum dipole based on the formula proposed by Shitov (1983) are underestimated by two orders of magnitude.

*Subject headings:* pulsars: general

---

<sup>1</sup>NAS-NRC Research Associate, on leave from Nicolaus Copernicus Astronomical Center, Toruń, Poland

## 1. Introduction

Since the discovery of pulsars (Hewish et al. 1968) the geometry of radio emission from pulsar magnetospheres was interpreted in terms of emission from purely dipolar magnetic fields (eg. Radhakrishnan & Cooke 1969; Cordes 1978; Lyne & Manchester 1988; Blaskiewicz et al. 1991; Rankin 1993; Gil & Kijak 1993). This assumption is justified by relatively high emission altitudes in comparison with  $R_{\text{ns}}$  inferred for the radio emission ( $\sim 0.01R_{\text{lc}}$ , where  $R_{\text{lc}} = cP/2\pi$  is the light cylinder radius and  $P$  is the rotation period of a neutron star with radius  $R_{\text{ns}}$ ). Most importantly, however, radio emission from the dipolar magnetic field hopefully can be described by a sufficiently small number of parameters and a limited number of observational parameters. The word “hopefully” reflects a second crucial assumption applied for the radio emission beam: that distinguishable features in pulse profiles (conal components, the outer edges of a profile) are associated with the beam structure (eg. of concentric hollow cones of enhanced radio emission) which in the reference frame corotating with the neutron star (CF) is symmetric with respect to the plane containing the dipole magnetic moment  $\vec{\mu}$  and the rotation axis. Without this disputable assumption, the number of parameters required to determine the emission geometry increases considerably and one is left with a multi-parameter theory to be compared with data from which only a few parameters can be deduced. Hereafter, the axial symmetry (in CF) of the radio emission beam is assumed; the problem of its justification is presented in Section 4.1.

To further constrain the parameter space, these two assumptions (I – dipolar magnetic field; II – symmetry of radio beam) are often supplemented with two additional simplifications: III – it is assumed that the bulk of radio waves is emitted in the direction which is tangent to the local magnetic field at an emission point. Given the large Lorentz factors of radio emitting electrons ( $\gamma \sim 10^2 - 10^3$ , eg. Ruderman & Sutherland 1975) this assumption should be fulfilled at least with accuracy of  $\sim 0.5^\circ$ . IV – identifiable features in pulse profiles (eg. maxima of conal components) observed at narrow frequency band are interpreted as radiation from very narrow range of altitudes. With the assumptions I–IV, the radio emission geometry becomes completely determined by four parameters:  $\alpha$ ,  $\beta$ ,  $r_{\text{em}}$ , and  $\rho$ . Their meaning is the following:  $\alpha$  is an inclination of the magnetic dipole with respect to the rotation axis (ie. the angle between the magnetic moment  $\vec{\mu}$  and the angular velocity  $\vec{\Omega} = 2\pi P^{-1}\hat{z}$ ).  $\beta$  is an “impact angle”, ie. the minimum angle between an observer’s line of sight and  $\vec{\mu}$ . This parameter is often replaced by  $\zeta = \alpha + \beta$  – the angle between the observer’s line of sight and the rotational axis. The next parameter,  $r_{\text{em}}$ , is the radial distance of radio emission region measured from the center of the neutron star. Hereafter, we will often use its normalized value  $r'_{\text{em}} = r_{\text{em}}/R_{\text{lc}}$ . The last parameter,  $\rho$ , is the half opening angle of the radio emission cone/beam, ie. it is the angle between the direction of radio emission in CF and  $\vec{\mu}$ . These four parameters determine completely the emission geometry in the sense that

any additional information about the emission region (eg. coordinates of emission point in the dipole frame, with z-axis along  $\vec{\mu}$ ) can be easily derived from textbook equations for the dipole geometry and spherical trigonometry.

One desired additional piece of information is an answer to the question “from which magnetic field lines does the observed emission come from?”. Following standard conventions, we identify magnetic field lines by  $\theta_{\text{fp}}$  – the colatitude of foot points of the magnetic field lines at the neutron star surface. With the radio emission altitude  $r_{\text{em}}$  and the beam radius  $\rho$  determined, the value of  $\theta_{\text{fp}}$  can be easily calculated. The parameter  $\theta_{\text{fp}}$  is often expressed in terms of a fraction of the polar cap angle:  $\theta'_{\text{fp}} = \theta_{\text{fp}}/\theta_{\text{pc}}$ , where  $\theta_{\text{pc}} = \arcsin((R_{\text{ns}}/R_{\text{lc}})^{1/2})$ .

These four quantities are to be deduced from radio data. In many cases, however, the data provide us with only two quantities:  $\beta$ , and  $W(f)$ , where  $W(f)$  is the apparent width of the radio pulse profile, usually defined by some simple criterion (eg. measured at some fraction  $f$  of maximum intensity; a wide variety of  $f$  is employed:  $f = 0.0005$  (Kijak & Gil 2003),  $f = 0.1$  (Blaskiewicz et al. 1991),  $f = 0.5$  (Rankin 1993),  $f = 1$  (Gangadhara & Gupta 2001)). The value of the inclination angle  $\alpha$  could in principle be determined along with  $\beta$  from the “rotating vector” model of polarization position angle swings (Radhakrishnan & Cooke 1969). In practice, however, a fit of the model to the observed position angle curve is much less sensitive to  $\alpha$  than to  $\beta$  (Rankin 1993). Only in exceptional cases can both these parameters be derived (Lyne & Manchester 1988; Blaskiewicz et al. 1991; Hoensbroech & Xilouris 1997). This led to a formulation of rather questionable methods of determining  $\alpha$  (Lyne & Manchester 1988; Rankin 1990). Some of their shortcomings will be discussed in Section 4.

Even accepting the questionable inclination angles, we are provided with three parameters ( $\alpha$ ,  $\beta$ ,  $W$ ), instead of the needed four. This situation gave birth to two kinds of methods for determining radio emission geometry: 1) A purely geometrical method which assumes that the lowest detectable emission at the leading and at the trailing edge of a radio pulse originates at the last open magnetic field lines, with  $\theta_{\text{fp}} = \theta_{\text{pc}}$ . With the fourth parameter assumed a priori, the method makes it possible to determine the radial position of radio emission  $r_{\text{em}}$  from the observed pulse width  $W_0$  (eg. Kijak & Gil 1997; 1998; 2003; Kijak 2001; hereafter we will use the index ‘0’ to refer to the pulse with  $W(f)$  at the lowest intensity level, ie. practically at  $f = 0.0005 - 0.1$ ). The derived altitudes are a few tens of  $R_{\text{ns}}$  at observation frequency  $\nu \sim 1$  GHz. 2) Methods of the second kind are able to derive the fourth observational parameter by a measurement of phase shifts of some profile features with respect to some fiducial points. The methods are relativistic in the sense that the phase shifts are caused by combined effects of aberration and propagation time delays due to the finite speed of light  $c$  (for brevity, the latter effect will hereafter be called retardation). The

second methods are superior to the geometric method in that they do not assume a priori the value of the fourth parameter. However, they must rely on additional assumptions about the radio pulse profile. Gangadhara & Gupta (2001, hereafter GG2001) measure the relativistic phase shift of conal components with respect to the core component, which is assumed to originate from much lower altitude than the cones which surround it. Blaskiewicz et al. (1991, hereafter BCW91) measure the shift of pulse edges with respect to the center (or the “inflection point”) of the position angle curve which is assumed to originate from the same altitude as the emission at the outer wings of the profile. On average, the method of Blaskiewicz et al. (1991) (hereafter BCW method) gives emission radii in rough agreement with that of the geometric method (Gil & Kijak 1993; Kijak & Gil 1997; 1998; 2003). The method of GG2001 predicts notably larger  $r_{\text{em}}$  – two times (or even more) larger than the geometric values. This discrepancy is not fatal for the model of GG2001, since it does not refer to the outer edge of pulse profiles. Nevertheless, part of this discrepancy will be removed in Section 2. Unlike the geometric method (eg. Gil & Kijak 1993), both relativistic methods (of GG2001 as well as BCW91) *in principle* make it possible to identify the radio emitting field lines. GG2001 and Gupta & Gangadhara (2003, hereafter GG2003) find  $\theta'_{\text{fp}}$  in the range  $0.22 - 0.74$  for radio emission observed at maxima of conal components. Unfortunately, the method of GG2001 can be applied only for pulsars having unambiguously identifiable pairs of conal components (and which possess a core component). So far, this has required application of a window thresholding technique (hereafter WT technique, GG2001) and limited application of the method only to a handful of the brightest objects. On the other hand, the BCW method suffers from difficulty in finding the center of the position angle curve, and, as we show below, it yields values of  $\theta'_{\text{fp}}$  exceeding 1. For convenience, hereafter we refer to the relativistic methods of GG2001 and BCW91 with the term “relativistic phase shift methods” (RPS methods).

In Section 2 we correct the method of GG2001, which results in a new formula for radio emission altitudes and furnishes the method with new interesting features. In Section 3 we propose to apply the method to the outer edges of averaged pulse profiles. This will hopefully provide a test of the main assumption of the geometrical method about the value of  $\theta'_{\text{fp}} = 1$  for the beam edge. As an example, we try to perform such a test using the method of BCW91. In Section 4 we discuss in detail weak points of the relativistic methods. Our conclusions are in Section 5.

## 2. Correction of the method of Gangadhara & Gupta

The RPS method of Gangadhara & Gupta (2001) applies to pulsars with both core and cone emission, ie. for M and T pulsars in classification scheme of Rankin (1993). Questionability of the conal pattern of radio emission beam will be discussed in Section 4.1. The model assumes the following: 1) the altitude of core emission is much lower than the altitude of conal emission (see Section 4 for arguments and counterarguments); 2) in the reference frame corotating with the neutron star the cones are symmetric around the narrow core beam. Obviously, in the case of the dipolar magnetosphere the second assumption can be most naturally accounted for by a model of the radio beam consisting of a narrow core beam centered at the dipole axis and a few nested hollow cones of enhanced radio emission surrounding the core. Magnetic field lines corresponding to a given cone have the same  $\theta_{\text{fp}}$  and the same half-opening angle  $\rho$  at a fixed altitude. In fact, the second assumption can be made less stringent: it is sufficient for the conal beams to be symmetric with respect to the plane containing the core component and the rotation axis. Thus, the “conal” beams may have eg. elliptical crosssection with the core beam located in the plane containing the ellipse center and the rotation axis (ie. not necessary at the ellipse center). The possibility of the elliptic beam is discussed eg. in Mitra & Deshpande (1999).

The method starts with identifying the core component in the radio pulse profile. Then one attempts to identify the same number of conal components on both the leading and the trailing side of the core component. The innermost pair of two conal components located on both sides of the core is identified as emission from the same, innermost hollow cone of radio beam. The next pair of conal components which bracket/flank the innermost pair is interpreted as emission from the next-to-innermost hollow cone of the radio beam, and so on. For each conal pair the observed phase of the leading component ( $\phi_l$ ) and the phase of the trailing component ( $\phi_t$ ) is measured with respect to the core component which defines the phase  $\phi = 0$ . As emphasized by GG2003 in all cases with clear identification of cones, the conal components were shifted toward earlier phases with respect to the core component, ie.  $|\phi_l| > \phi_t$ . This effect was noticed already by Gil (1985), who proposed the retardation effect to explain the asymmetry. More correctly, GG2001 interpreted the asymmetry as a forward shift of conal components due to combined effects of aberration of conal emission and retardation of core emission. We denote the (negative) relativistic phase shift between the midway point of conal pairs and the core component by  $\Delta\phi$ .

As long as the assumptions 1 and 2 are fulfilled, an observer detects the radio emission from the leading and from the trailing part of a cone at phases  $\phi_l$  and  $\phi_t$  given by

$$\phi_l = -\phi_0 + \Delta\phi; \quad \phi_t = \phi_0 + \Delta\phi, \quad (1)$$

where  $\phi_0$  is the phase of the trailing conal component (and  $-\phi_0$  is the phase of the leading conal component) in the absence of aberration and retardation (GG2001). Since both  $\phi_l$  and  $\phi_t$  can be measured, the two equations make it possible to calculate the relativistic shift  $\Delta\phi$  and  $\phi_0$ :

$$\Delta\phi = \frac{\phi_t + \phi_l}{2}; \quad \phi_0 = \frac{\phi_t - \phi_l}{2}. \quad (2)$$

The observed positions of the two components ( $\phi_l$  and  $\phi_t$ ) measured with respect to the core component are the *two* most desired observational parameters which replace the single  $W$  parameter (in the case considered here  $W = 2\phi_0$ ). Beyond question, recognizing this point is a great insight of Gangadhara & Gupta (2001).

The next step in the method of GG2001 was to express  $\Delta\phi$  in terms of radial distance of radio emission  $r_{\text{em}}$ . The value of  $\Delta\phi$  is a sum of a shift due to the aberration and a shift due to the retardation:  $\Delta\phi = \Delta\phi_{\text{ab}} + \Delta\phi_{\text{ret}}$ . The retardation shift is equal to

$$\Delta\phi_{\text{ret}} \simeq -\frac{r_{\text{em}}}{R_{\text{lc}}}, \quad (3)$$

regardless of  $\alpha$  and  $\beta$ , at least as long as the lowest order ( $\sim r'_{\text{em}}$ ) relativistic effects are considered.

The aberration changes the direction of photon emission by an angle:

$$\eta_{\text{ab}} \simeq \frac{v_{\text{rot}}}{c} \simeq \frac{r_{\text{em}}}{R_{\text{lc}}} \sin \zeta \quad (4)$$

where  $\vec{v}_{\text{rot}} = \vec{\Omega} \times \vec{r}_{\text{em}}$  is the local corotation velocity at the emission point (Cordes 1978; Phillips 1992; GG2001). The aberration throws photons forward, ie. in the direction of  $\vec{v}_{\text{rot}}$  and, to first order in  $r_{\text{em}}/R_{\text{lc}}$ , the angle between the non-aberrated and the aberrated emission direction is given by equation (4).

However, the resulting phase shift  $\Delta\phi_{\text{ab}}$  is *not* equal to  $-\eta_{\text{ab}}$  (contrary to what is argued in GG2001) just because the aberrated emission direction, when rotated by  $360^\circ$  around  $\vec{\Omega}$ , does not delineate a great circle on a sphere centered at the star. For this reason, the aberrational shift can be approximated by:

$$\Delta\phi_{\text{ab}} \simeq -\frac{\eta_{\text{ab}}}{\sin \zeta} \simeq -\frac{r_{\text{em}}}{R_{\text{lc}}}. \quad (5)$$

Thus, the total relativistic shift is equal to  $\Delta\phi \simeq -2r'_{\text{em}}$ , and the resulting formula for the emission radius is

$$r_{\text{em}} \simeq -\frac{\Delta\phi}{2}R_{\text{lc}}. \quad (6)$$

The formula gives emission radii smaller by a factor  $a \simeq (1 + \sin \zeta)/2$  than those obtained by GG2001 (cf. their eq. (9)). For objects with moderate or large dipole inclinations ( $\alpha \simeq 40^\circ - 90^\circ$ ) this is barely a cosmetic correction, however, for nearly aligned rotators the radii become almost two times smaller. The method of GG2001 applies to pulsars with well resolved conal components. This criterion favours objects with small  $\alpha$ , and, therefore, makes the correction important. GG2003 find particularly large emission radii for two objects, one of which (B2111+46) has very small inclination angle  $\alpha = 9^\circ$ . For this object, viewed at the angle  $\zeta = 11.4^\circ$ , our correction results in emission radii which are smaller by a factor of 0.6 than those derived by GG2003. For the second problematic pulsar (B2045–16), viewed at a considerably larger angle  $\zeta = 37.1^\circ$ , our correction does not reduce the radii significantly. GG2003 report some difficulties with unambiguous identification of conal pairs for this pulsar. Using values of  $\phi_l$  and  $\phi_t$  published by GG2001 and GG2003 we recalculated the radio emission radii for objects studied therein. Correct values are given in Table 1 (columns 5 and 6).

We emphasize that our correction is not barely a rescaling of the method of GG2001, but it furnishes their method with completely new features. Unlike the original equation (9) of GG2001, our formula for the emission radius (6) *does not* depend on  $\alpha$  and  $\beta$ , which is a precious feature given the problems with determining  $\alpha$ . A method of BCW91 is also independent on  $\alpha$  and  $\beta$ , however, it requires polarization measurements, and can only be applied to pulsars with well ordered position angle swings. Our correction of the method of GG2001 provides a method for determining  $r_{\text{em}}$ , which not only can do without the knowledge of  $\alpha$  and  $\beta$ , but at the same time it does not require the polarization measurements. It is based solely on information contained in M, and T-type profiles. We warn that the above described “not a great circle” error is also present in other papers (eg. Phillips 1992) and can be traced back in time at least to the paper of Cordes (1978). The paper of BCW91 is free from this error. The relativistic phase shift calculated in their paper is in full agreement with our formula (6) (cf. BCW91, p. 649). As argued in BCW91, the approximation (6) holds with accuracy of  $\sim 10\%$  for  $r'_{\text{em}} \lesssim 0.01$  if rotational distortions of the magnetic field from the dipole shape are negligible, but see Section 4.1 for a revision of this assumption.

To identify magnetic field lines from which the conal emission originates, it is necessary to determine the half opening angle  $\rho$  of the emission cones. This is accomplished with the help of a cosine formula of spherical trigonometry, which connects the values of  $\rho$ ,  $\alpha$ , and  $\zeta$  with the observed separation of conal components  $W(f = 1) = 2\phi_0$ :

$$\cos \rho = \cos \phi_0 \sin \alpha \sin \zeta + \cos \alpha \cos \zeta. \quad (7)$$

This time the knowledge of  $\alpha$  and  $\zeta$  is necessary. Since the formula for  $\rho$  does not depend on  $r_{\text{em}}$  the values of  $\rho$  calculated by GG2001 and GG2003 are correct.

With  $\rho$  and  $r_{\text{em}}$  determined, one can calculate the colatitude of footprints of active magnetic field lines at the star surface with the dipolar formula:

$$\theta_{\text{fp}} = \arcsin \left[ \left( \frac{R_{\text{ns}}}{r_{\text{em}}} \left( \frac{2}{3} - \frac{1}{6} \left( x + (x^2 + 8x)^{1/2} \right) \right) \right)^{1/2} \right], \quad (8)$$

where  $x = \cos^2 \rho$ . In the small angle approximation ( $\rho \ll 1$ ) the formula reduces to the well known approximate form:

$$\theta_{\text{fp}} \simeq \frac{2}{3} \rho \left( \frac{R_{\text{ns}}}{r_{\text{em}}} \right)^{1/2}. \quad (9)$$

Obviously, since the corrected method predicts lower emission radii than its original version but the same opening angles  $\rho$ , it must yield larger footprint colatitudes  $\theta_{\text{fp}}$ . Since,  $\theta_{\text{fp}} \propto r_{\text{em}}^{-1/2}$  the values of  $\theta_{\text{fp}}$  increase only by a factor of  $b = (2/(1 + \sin \zeta))^{1/2}$  between 1 and 1.4. Correct values of  $\theta'_{\text{fp}} = \theta_{\text{fp}}/\theta_{\text{pc}}$  for objects studied by GG2001 and GG2003 are given in the last column of Table 1. They range from 0.28 to 0.88. The values of  $\theta'_{\text{fp}}$  for the outermost cones cover the range between 0.35 and 0.88. Errors of  $\theta'_{\text{fp}}$  are based only on errors of  $\phi_l$  and  $\phi_t$  determined by GG2001 and do not include the large uncertainties of  $\alpha$ , and  $\beta$ .

Since our correction rescales the values of  $r_{\text{em}}$  and of  $\theta_{\text{fp}}$  by factors which are the same for a given pulsar, the main findings of GG2001 and GG2003 (ie. higher altitudes for broader cones and lower altitudes for higher radio frequencies) remain valid.

### 3. Comparison of the RPS methods with the geometrical method

In addition to the conal components, there is one more feature in radio pulse profiles which for a long time has been believed to be symmetric with respect to the  $(\vec{\Omega}, \vec{\mu})$  plane – the outer edge of the radio beam. The assumption about the symmetry has always been present in the traditional, geometric method of determining radio emission altitudes (eg. Kijak & Gil 1997). For example, Kijak & Gil (2003) emphasize that “it is important for our method that an apparent pulsar beam spreads out about equally at both sides of the so-called fiducial plane, containing both the rotation and the magnetic axis”. Also, it has always been assumed



in the method that both the leading and the trailing side of the edge originates from the same altitude. If assumption 1 of the method proposed by GG2001 also applies to the outer edge of the beam (ie. if the “edge emission” originates from much higher altitudes than the core emission), the method of GG2001 may also be applied to the edges of radio beam, not only to maxima of the conal components. Hereafter, the RPS method of GG2001 with this assumption will be referred to as the “outer edge relativistic phase shift method” (OERPS method). The method requires a measurement of  $\phi_l$  and  $\phi_t$  for the outer edges of an *averaged* pulse profile. Then calculations of the original method of GG2001 can be performed (equations 1 – 8) to determine both the altitude and the locations of magnetic field lines for the radio emission at the pulse edge.

The OERPS method does not require an identification of conal components within the pulse profile. This method will work without the analysis of single pulses (with the WT technique) and it can be applied directly to averaged pulse profiles with large signal to noise ratio. This application of the OERPS method may seem undesirable because it provides  $r_{\text{em}}$  and  $\theta_{\text{fp}}$  for the lowest intensity radio emission at the threshold of detection. However, when applied in this way, the OERPS method may serve as a test of the geometric method. As emphasized by Kijak & Gil (2003), in the geometric method “the last open field lines are believed to be associated with the lowest detectable level of radio emission at the profile wings”, ie.  $\theta'_{\text{fp}} = 1$  is assumed. This crucial assumption of the geometric method is its weak point and, therefore, proving or disproving it is an important task. As Kijak & Gil admit “it is possible that a forbidden area exists at the outer parts of the polar cap. Evidently, we cannot give a theoretical answer to these questions.” The application of the OERPS method to the outer edge of the radio pulse may give some insight into the problem.

Because we have no access to high-quality radio data to apply the OERPS method, instead, below we try to use the BCW method to identify the active magnetic field lines. Like the OERPS method, the method of BCW91 provides the value of  $r_{\text{em}}$  in a way which is independent of  $\alpha$ ,  $\beta$ , and, most importantly, of  $\theta_{\text{fp}}$ . The lowest intensity half width  $W_0$  (usually measured by Blaskiewicz et al. (1991) at the level of  $f = 0.02$  and used to determine the center of a profile) is equal to  $\phi_0$  which, along with  $\alpha$ ,  $\beta$ , and  $r_{\text{em}}$ , provides all necessary information to calculate  $\theta_{\text{fp}}$  with the help of equations (7) – (8), ie. in the same way as in GG2001. The BCW method has been used to determine  $r_{\text{em}}$  by von Hoensbroech & Xilouris (1997) (hereafter HX97). They note that the method requires neither the knowledge of the viewing geometry ( $\alpha$ ,  $\beta$ ) nor the physical boundaries of radiation zones ( $\theta_{\text{fp}}$ ) and emphasize that this is its significant advantage over the geometric method. BCW91 and HX97 limited their application of the BCW method to calculations of  $r_{\text{em}}$ . Going just one step further one can determine the surface colatitude  $\theta_{\text{fp}}$  of the magnetic field lines associated with the lowest-intensity level at the outer edges of pulse profiles. Normally, this would require using

the equations (7) – (8) with  $\phi_0 = W_0/2$ . An easier way is to use the equation (9) which implies that the ratio of  $\theta_{\text{fp}}$  calculated with the BCW method, and the geometric method is:

$$\frac{\theta_{\text{fp,BCW}}}{\theta_{\text{fp,geo}}} \simeq \left( \frac{r_{\text{geo}}}{r_{\text{delay}}} \right)^{1/2} \simeq \theta'_{\text{fp,BCW}}, \quad (10)$$

because  $\theta_{\text{fp,geo}} = \theta_{\text{pc}}$  by assumption, which we want to verify. In the above formula  $\theta_{\text{fp,BCW}}$  and  $r_{\text{delay}}$  refer to the values of  $\theta_{\text{fp}}$  and  $r_{\text{em}}$  obtained with the BCW method, whereas  $\theta_{\text{fp,geo}}$  and  $r_{\text{geo}}$  refer to the geometric method (Gil & Kijak 1993; Kijak & Gil 1997; 1998; 2003). We use the values of  $r_{\text{delay}}$  and  $r_{\text{geo}}$  calculated for the same data set by BCW91 and presented in their table 3. We do not analyse the results of HX97 since the authors have not taken into account errors of  $\alpha$  and  $\beta$  in calculation of  $r_{\text{geo}}$ , which would result in overestimating the accuracy of  $\theta_{\text{fp}}$ . BCW91 studied 35 cases, where by ‘the case’ we mean a determination of  $r_{\text{delay}}$  and  $r_{\text{geo}}$  at a single frequency, so that one pulsar may comprise a few cases. Out of these, only 7 cases allow determination of  $\theta_{\text{fp}}$ . The other 28 cases would provide very little information or might be even misleading about the status of  $\theta_{\text{fp}}$ : Some of them exhibit strong asymmetry of pulse profiles indicating a lack of a leading/trailing component, other exhibit strong distortions of the position angle curve. For some of them the dipole inclination angle is unconstrained and only an upper limit for  $r_{\text{geo}}^{\text{max}}$  is available. Out of these cases we included only one (B1914+13), for which  $r_{\text{delay}} > r_{\text{geo}}^{\text{max}}$  which provides an upper limit for  $\theta_{\text{fp}}$ . Finally, some cases were excluded because of errors of  $r_{\text{delay}}$  exceeding 100%. Including all these cases would either provide no definite information about  $\theta_{\text{fp}}$  because of huge errors, or the information provided would be highly questionable, as in the case of the one-sided cones.

The values of  $\theta'_{\text{fp}}$  derived with the BCW method for the seven clean-cut cases with reasonably small statistical errors, and most probably free from systematic errors, are presented in column 3 of Table 2. Column 4 presents a range of  $\theta'_{\text{fp}}$  allowed by  $1\sigma$  errors derived for  $r_{\text{delay}}$  and  $r_{\text{geo}}$  by BCW91 (table 3 therein). The last column shows the level of consistency of the two methods (in  $\sigma$ ), ie. the level at which the derived values of  $\theta'_{\text{fp}}$  are consistent with 1.

A glance at values of  $\theta'_{\text{fp}}$  in Table 2 reveals that for four cases (B0301+19 and B0525+21, both at 0.43 and 1.4 GHz) the model yields  $\theta'_{\text{fp}} > 1$ , ie. radio emission from the closed magnetic field line region. The inconsistency with  $\theta'_{\text{fp}} = 1$  is at  $\sim 2\sigma$  level. This may be related to the problem of establishing to which parts of pulse profile the emission radii  $r_{\text{delay}}$  refer. In the method of BCW91, the values of  $r_{\text{delay}}$  are derived from the relative position of the outer edges of the profile and the center of the position angle (PA) curve. Let us assume that the center of the PA curve is determined mostly by the central parts of profiles which may originate from lower altitudes than the beam edge, according to the rule ‘inner means

lower’ (eg. Rankin 1993; GG2001). Accounting for this, BCW91 noted that their emission radii  $r_{\text{delay}}$  “are averaged over all emitting regions”. Had the inner regions of pulse profiles indeed come from lower altitudes, the derived radii  $r_{\text{delay}}$  would be smaller than the radii  $r_{\text{edge}}$ , referring to the pulse edge only, but not more than by a factor of 2. This is because the rotation shifts the profile center toward early phases by  $-2r_{\text{edge}}/R_{\text{lc}}$ , where  $r_{\text{edge}}$  is the radial distance for emission at the edge of a pulse profile. At the same time, the rotation delays the center of the position angle swing by  $2r_{\text{in}}/R_{\text{lc}}$ , where  $r_{\text{in}}$  refers to the radiation from inner parts of the profile which determine the position of the center of the PA swing, according to our working hypothesis. For  $r_{\text{edge}} \sim r_{\text{in}}$ , the total shift is  $4r_{\text{edge}}/R_{\text{lc}}$ , as derived by BCW91. For the other limiting case  $r_{\text{edge}} \gg r_{\text{in}}$  the shift is two times smaller:  $2r_{\text{edge}}/R_{\text{lc}}$ , so in general the emission radii for the beam edge may be at most two times larger than  $r_{\text{delay}}$  derived by BCW91 for the case of  $r_{\text{edge}} \sim r_{\text{in}}$ . Taking this possibility into account, one could decrease the values of  $\theta'_{\text{fp}}$  in Table 2 at most by a factor of  $2^{-1/2}$ , since  $\theta_{\text{fp}} \propto r_{\text{em}}^{-1/2}$  (eq. 8). Because of the large error range for  $\theta'_{\text{fp}}$  (column 4 in Table 2), this would make *two* of the four problematic values consistent with 1 within the level of  $1\sigma$ . The other two values of  $\theta'_{\text{fp}}$  (for B0301+19 at 1.42 GHz and B0525+21 at 0.43 GHz) would still remain inconsistent with 1 at  $1\sigma$  level. Thus, contrary to the suggestion of BCW91 (p. 664), lower emission altitudes for the central parts of profiles are not able to remove the disagreement completely. Different locations of emission regions for the conal peaks and for the bridge between them have been proposed for the two pulsars based on different spectra and fluctuation properties (Backer 1973; Rankin 1983; BCW91). For B0525+21, BCW91 suggest contribution of quadrupole component of stellar magnetic field as a source of the error.

For the other two cases presented in Table 2 (B1913+16 at two frequencies)  $\theta'_{\text{fp}} \simeq 1$  within  $1\sigma$ . This may be considered surprising too, because the object has been classified as a triple core pulsar (T), and its position angle curve exhibits strong distortions within considerable fraction of pulse window (cf. fig. 17 in BCW91). Whereas strong discrepancy of  $\theta_{\text{fp}}$  from unity for this case would be reasonable, it does not occur.

For the last object in Table 2, BCW91 were able to determine only an approximate upper limit for  $r_{\text{geo}}$ . Since the value of  $r_{\text{delay}}$  exceeds the limit, an upper limit of 0.8 for  $\theta'_{\text{fp}}$  has been obtained. This is the only case (of single core type – S<sub>t</sub>), which *would* question the main assumption of the geometric method, if the BCW method was reliable when applied to individual objects. Obviously, this could equally well imply the inactivity of the outer part of the polar cap as our inability to detect the outer wings of radio profiles. In either case, the assumption that  $\theta'_{\text{fp}} = 1$  at the *observed* profile edge would be invalidated.

Thus, by selecting a sample of pulsars studied by BCW91 with the smallest statistical errors, and least probable to be affected by systematic errors, we find that the BCW method

implies the radio emission from the region of closed magnetic field lines, with  $\theta'_{\text{fp}} > 1$ , in some cases at the level  $> 2\sigma$ . This is in conflict with the stringent theoretical estimate of the angular size of the open field line region (eg. Ruderman & Sutherland 1975) and apparently questions application of the BCW method as a tool for determining  $\theta'_{\text{fp}}$  for individual objects.

As argued above, there is no reason for not applying the RPS method of GG2001 to the outer (or “lowest intensity”) edge of pulse profiles. The only additional assumption required to extend the method in this way is the necessity for the edge emission to come from much larger altitudes than the core. This seems reasonable since the outer edges of a profile are often associated with outer wings of the outermost conal components, which seem to originate from much larger altitude than the core (Rankin 1993; GG2003). It is possible that the method will provide more reliable way of determining  $\theta'_{\text{fp}}$  because it is less affected by the disordered polarization behaviour than the BCW method (the polarization affects the values of  $\beta$  and  $\alpha$ , required to calculate  $\theta'_{\text{fp}}$ , but not the measurement of the phase shift, although the latter is two times smaller than in the BCW method). Our estimates of  $\theta'_{\text{fp}}$  with the OERPS method for B0329+54 at 606 MHz, B1237+25 and B1857–26 at 318 MHz give  $\theta'_{\text{fp}} \simeq 1$ , in agreement with the assumption of the geometric method. These are based on rough “by eye” estimations of  $\phi_1$  and  $\phi_t$  from figures in GG2001 and GG2003, and we mention them just to show another possibility of determining  $\theta'_{\text{fp}}$  for the beam edge.

The method of BCW91 requires high-quality polarization measurements and can be applied only to pulsars with well ordered position angle swings, with cores or not. The OERPS method does not require polarization measurements, but can be applied only for pulsars with both core and cone emission (M and T). Since the presence of a core in pulse profiles is often accompanied by the disordered shape of position angle curve (eg. Rankin 1993), the two methods can complement each other. On the other hand, this is a disadvantage, because it makes it difficult to compare the methods. Such a comparison would be interesting because emission radii derived with both these methods do not suffer from uncertainties of  $\alpha$  and  $\zeta$ . So far the method of BCW has been “successfully” applied for only one object studied by Gangadhara & Gupta – B2045–16. Our rough estimate of  $r_{\text{em}}$  and  $\theta'_{\text{fp}}$  for the outer edge of pulse profile of this pulsar gives  $r_{\text{em}} \sim 2000$  km and  $\theta'_{\text{fp}} \sim 0.5$ . This is much larger than  $2r_{\text{delay}} = 886$  km derived by HX97 with the BCW method but this should be verified by detailed analysis.

A serious shortcoming of the OERPS method is that it requires very accurate measurements of the observed positions  $\phi_1$  and  $\phi_t$  of the leading and the trailing edge of a radio pulse profile. These are much less defined than the positions of conal maxima. Therefore, the method may give less accurate results than the original RPS method of GG2001, unless very precise determination of  $\phi_1$  and  $\phi_t$  is achieved. GG2001 and GG2003 found that shifts

of outermost cones’ maxima with respect to the core may in some cases be as large as  $3^\circ$ , and they were able to measure some shifts with accuracy of  $\sim 0.05^\circ$  ie. a few percent. A much larger error (typically  $\sim 30\%$ ) is inherent in the OERPS method and in the method of BCW91 which must deal with locating the “lowest intensity” points. Establishing accurate technique of determining positions of these points is crucial to improve the methods. As shown above, however, notable differences of  $\theta'_{\text{fp}}$  from unity *can* be detected despite the large statistical errors, and if the OERPS method is less sensitive to systematic errors than the BCW method it will provide a unique opportunity to test the main assumption of the geometric model and/or cross-comparison of the three methods.

## 4. Weak points of the relativistic phase shift methods

### 4.1. (A)symmetry of the radio beam

To provide reliable estimates of  $r_{\text{em}}$  the RPS method of GG2001 requires the symmetry of cones of enhanced radio emission with respect to the plane containing the core component and the rotation axis. To calculate  $\theta_{\text{fp}}$ , the core/cones system must be centered at the dipole axis. The OERPS method requires the same symmetry for the outer edge of the radio beam, and the BCW method requires the symmetry of the beam edge with respect to the the  $(\vec{\Omega}, \vec{\mu})$  plane, regardless of the position of the core component. All these assumptions are related to the old problem: is the beam shape conal or patchy? The patchy beam would invalidate all these methods. Fortunately, however, statistical analyses of distribution of components within the radio pulse provide arguments for the conal shape (eg. Mitra & Deshpande 1999; Kijak & Gil 2002). The work of Lyne & Manchester (1988) (hereafter LM88) provides little (or no) argument for the patchy shape. This is because central components of pulse profiles seem to originate from lower altitudes than the outer components (eg. Rankin 1993; GG2001). Aberration and retardation effects shift the relative positions of different components in phase by  $\Delta\phi \simeq 2\Delta r'_{\text{em}}$ , where  $\Delta r'_{\text{em}}$  is the difference of emission radii between different components in units of  $R_{\text{lc}}$ . Estimating  $\Delta r'_{\text{em}} \sim 0.01$  one obtains  $\Delta\phi \sim 1^\circ$  which amounts to  $\sim 13\%$  of pulse width observed for pulsars with large dipole inclinations ( $\alpha \sim 90^\circ$ ). Given that observed separation between components is much smaller than the pulse width (say  $20 - 40\%$ ), these shifts, different for different objects because of diversity of  $r_{\text{em}}$ , along with other factors (eg. inexactly determined impact angles  $\beta$ ) could easily produce the “essentially random” distribution of components within the pulse window, ie. in figures like the fig. 12 in LM88. It is very important, that the figure of LM88 shows projection of components on a circle representing 10% intensity level of pulse outer edges and does not reflect relative positions of the components in the reference frame corotating with the star. One trace of the

“mixing” introduced by aberration and retardation on such a “projection cap” should be an increased number of components on its trailing half, because the aberration and retardation squeezes the trailing half of a profile, and broadens the leading half, so that the profile center is slightly shifted toward early phases with respect to the core component. Why this effect is not visible in fig. 12 of LM88? Perhaps, because the figure includes a large diversity of profile types, many of which (eg.  $S_t$ ,  $S_d$ ,  $D$ , and  $cQ$ , using the classification terminology of Rankin 1993) should not contribute to the effect. Because the relativistic shift is smaller than the typical component separation, it is safe to assume that only the core component enters the trailing half of a profile, with the profile center corresponding to the midway point between the profile outer edges. Thus, in the case of the M profiles, with typically 5 components, the ratio  $R$  of the number of components within the trailing half to those within the leading half of the profile would be equal to  $3/2$ . For T profiles (core plus two conals) the ratio is 2, and it is the same for cT profiles provided that the inner cone originates from lower altitude than the outer cone. Only 14% of objects considered by LM88 were classified as M pulsars by Rankin (1993), 21.5% as T, and 3.3% as cT. This implies that the ratio  $R$  in fig. 12 of LM88 should be equal to 1.3 instead of the value of 0.95 which can be deduced from their figure (assuming that  $R = 1$  for 24% of nonclassified objects). Perhaps the difference can be attributed to the trend for the trailing conal components to be missing or to have lower intensity than the leading ones (LM88). Such one-sided conals would appear to have single profiles (identified as  $S_d$  or, incorrectly, as  $S_t$ ) with maximum shifted toward early phases, which would decrease  $R$ . It would be interesting to prepare a figure similar to the fig. 12 of LM88, but including objects classified only as T and M. For 19 M pulsars and 49 T pulsars classified by Rankin (1993) the ratio of components’ number within each half of the “projection cap” should be as high as  $R \simeq 1.86$ . This would support the relativistic interpretation of profile’s asymmetry, ie. the importance of aberration and retardation effects.

Other arguments for the conal beam shape are provided directly by the WT technique of GG2001. For 6 (out of 7) objects studied by GG2001 and GG2003, the same number of conal components was found on both sides of the core component, and only B2045–16 is *possible* exception. In all cases, strong (ie. easily identifiable) components on the leading side corresponded to strong components on the trailing side, whereas new weak components, detected with the WT technique on one side of the core were always associated with weak components on the other side. It is natural to interpret this coincidence in terms of the conal, not patchy beam shape. Another interesting implication of this relation is the possibility of applying the method of GG2001 to a larger number of T and M pulsars, without the necessity of identification of all cones with the WT technique.

Thus, the conal beam shape seems to be consistent with observations. On theoretical

grounds, the conal shape is supported by a model of sparks rotating around the magnetic pole due to the  $\vec{E} \times \vec{B}$  drift (Ruderman & Sutherland 1975; Gil & Sendyk 2000). The model, as well as the conal beam hypothesis, is supported by observations of subpulse drifts (Gil & Krawczyk 1997; Deshpande & Rankin 1999; Vivekanand & Joshi 1999). How exact the symmetry of the cones can be, however? The relativistic phase shift methods are based on a measurement of very small phase shifts  $\sim r_{\text{em}}/R_{\text{lc}} \sim 0.01$  rad and, therefore, it is crucial to give precise answer this question. The symmetry of the radio beam is determined by the symmetry of the magnetic field within the emission region. Assuming that  $r_{\text{em}}$  is sufficiently high for quadrupole components of the stellar magnetic field to be negligible, one must still consider distortions  $\Delta\vec{B}$  of the dipolar field due to the rotation and magnetospheric currents. The currents are estimated to modify  $\vec{B}$  by a factor of higher order than  $\beta_{\text{rot}} = v_{\text{rot}}/c \sim r_{\text{em}}/R_{\text{lc}}$  (eg. for longitudinal currents  $|\Delta\vec{B}| \sim \beta_{\text{rot}}^{3/2}$ , BCW91; Dyks & Rudak 2002). Estimates of magnitude of the rotational distortions, unfortunately, are far from consistency. Eg. Shitov (1983) estimates  $|\Delta\vec{B}| \sim \beta_{\text{rot}}^3$ , whereas Arendt & Eilek (1998) find much larger value of  $|\Delta\vec{B}| \sim \beta_{\text{rot}}$ . According to the estimate of Shitov (1983), the rotational distortions are completely negligible in comparison with the effects of aberration and retardation ( $\sim \beta_{\text{rot}}$ ). This argument has been commonly used to justify the static dipole approximation (eg. BCW91; GG2001).

In Fig. 1 we present the radio beam shape calculated according to the exact expression for the vacuum dipole distorted by the rotation (eg. Cheng et al. 2000) at altitude of  $r_{\text{em}} = 0.01R_{\text{lc}}$ . More precisely, the figure presents a crosssection of the last open field lines with a star-centered sphere of radius  $0.01R_{\text{lc}}$ . The last open field lines are those lines which are tangent to the light cylinder. Different panels correspond to different dipole inclinations  $\alpha$ . For a reference, a circular polar cap for a “star” with a radius  $0.01R_{\text{lc}}$ , centered at the magnetic moment axis, is overplotted in each panel (thin solid line; the angular radius of the cap is  $\theta_{01} \simeq 5.7^\circ$ ). Rotation is to the left, and the nearest pole is up. The figure clearly shows that the rotational distortions are large for  $\alpha \gtrsim 30^\circ$  and, unfortunately, asymmetric with respect to the  $(\vec{\Omega}, \vec{\mu})$  plane (a vertical at  $x = 0$ ). The asymmetry amounts up to  $0.2\theta_{01} \simeq 1^\circ$ , ie. it is comparable to the shift due to the aberration and retardation ( $\Delta\phi \sim 2r_{\text{em}}/R_{\text{lc}} \sim 1^\circ$ ). The exact magnitude of the asymmetry depends on the impact parameter  $\beta$ . Thus, the crucial assumption of the RPS methods does not have to be true: at least in the case of the *vacuum* dipole the rotational distortions of the beam are able to compete with aberration and retardation. Fig. 1 proves that estimates of rotational distortions of the radio beam shape based on Shitov’s formula are underestimated by two orders of magnitude. We emphasize that we consider just distortions of the outer edge of the radio beam at fixed altitude, not of magnetic field lines which, in principle, could stay practically undisturbed at low altitudes. Results similar to those in Fig. 1 have been obtained by Romani & Yadigaroglu (1995),

Arendt & Eilek (1998), and Cheng et al. (2000), although the authors did not determine the shape of the “beam rim” near a notch which can be seen in Fig. 1 for moderate inclination angles  $\alpha \simeq 40^\circ - 50^\circ$  (eg. Arendt & Eilek incorrectly suggest that the rim is discontinuous at the notch).

The contours shown in Fig. 1 present the radio beam boundaries for the *vacuum* dipole, ie. they do not have to approximate the actual shape of the beam. Indeed, loading the magnetosphere with charge-separated plasma, and assuming no longitudinal currents, recovers the symmetry of the beam with respect to the  $(\vec{\Omega}, \vec{\mu})$  plane (eg. Beskin et al. 1993). Allowing for longitudinal currents, and including the particle inertia would result in a beam shape which still awaits to be derived, but most probably would differ much from the one shown in Fig. 1. Therefore, Fig. 1 does not invalidate the RPS methods, but indicates potential problems. The suggested ubiquity of *forward* shift of conal components with respect to the core (Gil 1985; GG2001), if confirmed, would provide argument for aberration and retardation being dominant effects.

#### 4.2. The reference altitude

All RPS methods rely on a measurement of a shift between three identifiable points within a pulse profile and make assumptions about relative altitudes of these points. The method of GG2001 assumes that radiation at conal maxima comes from much larger altitudes than the core emission. As noted by GG2003, if this is not the case, the emission radii  $r_{\text{em}}$  derived with their method should be treated as lower limits, or in case the radial distance of core emission is known, it should be added to  $r_{\text{em}}$ . The same is true for the OERPS method applied to the beam edge. PSR B0450–18, studied by GG2003, provides an example of a profile, for which the central (core?) component comes from high altitudes. Also, it illustrates some shortcomings of the method of determining  $\alpha$  proposed by Rankin (1990). The pulsar is viewed at so large impact angle ( $\beta \simeq 4^\circ$ ) that any core emission from the near surface region, with opening angle  $1.5\theta_{\text{pc}} \simeq 1.68^\circ$ , should be missed by the line of sight. If the value of  $\beta$  is correct, the central component must be either a higher-altitude core component or an inner cone component, as suggested by GG2003. To maintain the estimated width of  $\sim 8^\circ$  (Rankin 1993), the component would have to originate from radial distance  $r_{\text{em}} \simeq 67$  km, assuming  $\alpha = 24^\circ$ ,  $\beta = 4^\circ$  and  $\theta'_{\text{fp}} = 1$  as in Rankin (1990); (Rankin assumes  $\theta'_{\text{fp}} = 1$  for the full width at half maximum of the “core” component at 1GHz). This value is larger than the error of  $r_{\text{em}}$  estimated for this object in Table 1 and should be added to  $r_{\text{em}}$ . However, the value of  $\alpha$  derived for this object with Rankin’s method based on  $W(f = 0.5) \sim 8^\circ$  and  $P = 0.55$  is questionable because the measured impact angle  $\beta$  is not consistent with



$r_{\text{em}} = 10 \text{ km}$  and  $\theta'_{\text{fp}} = 1$ , assumed in the derivation of  $\alpha$ .

The RPS method of BCW91 assumes that radio emission at the edge of a profile originates from *the same* altitudes as the emission which determines the center of the position angle curve, in which case the predicted shift is equal to  $4r_{\text{em}}/R_{\text{lc}}$ . As noted above this assumption, if not satisfied, would lead to an underestimate of emission altitudes for the outer edge of a profile.

Three objects studied by BCW91: B1913+16 (0.43 GHz, fig. 17 in BCW91), B1916+14 (1.4 GHz, fig. 20 in BCW91) and B2210+29 (0.43 GHz, fig. 26 in BCW91) have been classified by Rankin (1993) as T, T, and M-type pulsars, respectively. Therefore, they may serve as a cross-comparison test for all the three RPS methods, provided we do not mix conal components associated with different cones. In the case of B1913+16 and B2210+29 the position of the core component is shifted with respect to the position angle center by roughly the same value as the pulse edges. This would imply similar emission altitudes for both the core components and the beam edge (eg.  $\sim 150 \text{ km}$  for B1913+16, BCW91). Interestingly, for B1913+16 the conal maxima are shifted toward early phases with respect to the core, as if they originated from even higher altitude (by  $\sim 90 \text{ km}$ ) than the core/edge. For B1916+14 (fig. 20 in BCW91), the core component seems to slightly precede the profile center (ie.  $r_{\text{core}} \gtrsim r_{\text{edge}}$ ), although the conal maxima again seem to be shifted toward earlier phases with respect to the core, implying  $r_{\text{conal}} \gtrsim r_{\text{core}}$ . No such effects can be discerned in the 0.43 GHz pulse profile of B2210+29, though the center of its pulse is shifted with respect to the position angle center by a larger amount than in the case of B1916+14. This rough analysis indicate that  $r_{\text{delay}}$  of BCW91 method may have little to do with  $r_{\text{em}}$  derived with the method of GG2001, and that at least in some cases  $r_{\text{core}} \sim r_{\text{edge}}$ .

## 5. Summary

We corrected the relativistic method of GG2001 of determining the radio emission geometry within pulsar magnetospheres. The correction results in a method of determining the radio emission altitudes which does not depend on viewing geometry nor does it require polarization measurements. According to this method, the radial distance of the radio emission region in units of  $R_{\text{lc}}$  is equal to a half of the relativistic phase shift of a pair of conal components with respect to the core component. We propose to extend application of the method to the outer edge of radio pulse profiles to identify magnetic field lines associated with the edge. This may provide a test of the geometrical method of determining  $r_{\text{em}}$ , based on a measurement of a pulse width at the lowest intensity level.

We have tried to perform such a test using the relativistic method of Blaskiewicz et al. (1991). This has revealed that in individual cases the method often implies emission from the region of closed magnetic field lines. Following BCW91 we associate this with large systematic errors inherent to the method. The method is not accurate enough to identify the radio emitting magnetic field lines in individual objects.

Finally, we have shown that exact numerical calculations invalidate the estimate of rotational distortions of the *vacuum* magnetic dipole field, based on the formula of Shitov (1983). This does not have to be threatful for the relativistic methods of GG2001 and BCW91, because in the vicinity of the light cylinder the vacuum dipole does not have to be a good approximation of actual, plasma-filled magnetosphere. However, this indicates potential problems with the methods. Also, we determined the shape of the open field line region within a notch which appears for moderate dipole inclinations on the leading, pole-ward side of the region.

We thank U. Dyks for analysis of results of LM88. JD thanks V. S. Beskin for comments on pulsar magnetosphere. This work was performed while JD held a National Research Council Research Associateship Award at NASA/GSFC. The work was also supported by the grant PBZ-KBN-054/P03/2001 (JD and BR).

## REFERENCES

- [1998]Arendt, P. N., & Eilek, J. A. 1998, ApJ, submitted (astro-ph/9801257)
- [1973]Backer, D. C. 1973, ApJ, 182, 245
- [1993]Beskin, V. S., Gurevich, A. V., & Istomin, Y. N. 1993, “Physics of the Pulsar Magnetosphere”, Cambridge University Press, Cambridge
- [1991]Blaskiewicz, M., Cordes, J. M., & Wasserman, I. 1991, ApJ, 370, 643 (BCW91)
- [2000]Cheng, K. S., Ruderman, M. A., & Zhang, L. 2000, ApJ, 537, 964
- [1978]Cordes, J. M. 1978, ApJ, 222, 1006
- [1999]Deshpande, A. A., & Rankin, J. M. 1999, ApJ, 524, 1008
- [2002]Dyks, J., & Rudak, B. 2002, A&A, 393, 511
- [2001]Gangadhara, R. T., & Gupta, Y. 2001, ApJ, 555, 31 (GG2001)

- [1985]Gil, J. 1985, ApJ, 299, 154
- [1993]Gil, J. A., & Kijak, J. 1993, A&A, 273, 563
- [1996]Gil, J., & Krawczyk, A. 1997, MNRAS, 285, 561
- [2000]Gil, J. A., & Sendyk, M. 2000, ApJ, 541, 351
- [2003]Gupta, Y., & Gangadhara, R. T. 2003, ApJ, 584, 418 (GG2003)
- [1968]Hewish, A., Bell, S. J., Pilkington, J. D. H., Scott, P. F., & Collins, R. A. 1968, Nature, 217, 709
- [1997]von Hoensbroech, A., & Xilouris, K. M. 1997, A&A, 324, 981 (HX97)
- [2001]Kijak, J. 2001, MNRAS, 323, 537
- [1997]Kijak, J., & Gil, J. 1997, MNRAS, 288, 631
- [1998]Kijak, J., & Gil, J. 1998, MNRAS, 299, 885
- [2002]Kijak, J., & Gil, J. 2002, A&A, 392, 189
- [2003]Kijak, J., & Gil, J. 2003, A&A, 397, 969
- [1988]Lyne, A. G., & Manchester, R. N. 1988, MNRAS, 234, 477 (LM88)
- [1999]Mitra, D., & Deshpande, A. A. 1999, A&A, 346, 906
- [1992]Phillips, J. A. 1992, ApJ, 385, 282
- [1969]Radhakrishnan, V., & Cooke, D. J. 1969, Astrophys. Lett., 3, 225
- [1983]Rankin, J. M. 1983, ApJ, 274, 333
- [1990]Rankin, J. M. 1990, ApJ, 352, 247
- [1993]Rankin, J. M. 1993, ApJ, 405, 285
- [1995]Romani, R. W. & Yadigaroglu, I.-A., 1995, ApJ, 438, 314
- [1975]Ruderman, M. A., & Sutherland, P. G. 1975, ApJ, 196, 51
- [1983]Shitov, Y. P. 1983, Soviet Astr., 27, 314
- [1999]Vivekanand, M., & Joshi, B. C. 1999, ApJ, 449, 211

Table 1. Radial distances  $r_{\text{em}}$  of conal radio emission and surface colatitudes  $\theta'_{\text{fp}}$  of magnetic field lines associated with the cones derived with the relativistic phase shift method of GG2001 with the correction applied according to eq. (6) of Section 2. The numbers are based on cones’ shifts measured by GG2001 and GG2003 and  $\alpha$  and  $\beta$  values from Rankin (1993) (cf. table 1 in GG2001 and GG2002).

Pulsar	$P$ [s]	$\nu$ [MHz]	Cone <sup>a</sup>	$r_{\text{em}}$ [km]	$r_{\text{em}}$ [% of $R_{\text{lc}}$ ]	$\theta'_{\text{fp}}$
B0329+54	0.7145	325	1	$150 \pm 080$	0.44	$0.58 \pm 0.17$
		325	2	$330 \pm 060$	0.96	$0.57 \pm 0.06$
		325	3	$600 \pm 080$	1.74	$0.57 \pm 0.05$
		325	4	$880 \pm 240$	2.57	$0.65 \pm 0.12$
		606	1	$120 \pm 070$	0.35	$0.65 \pm 0.22$
		606	2	$280 \pm 050$	0.83	$0.58 \pm 0.06$
		606	3	$460 \pm 140$	1.35	$0.61 \pm 0.11$
		606	4	$640 \pm 180$	1.88	$0.71 \pm 0.12$
B0450–18 <sup>b</sup>	0.5489	318	1	$230 \pm 25$	0.88	$0.65 \pm 0.04$
B1237+25	1.3824	318	1	$160 \pm 40$	0.24	$0.34 \pm 0.06$
		318	2	$411 \pm 30$	0.62	$0.43 \pm 0.02$
		318	3	$540 \pm 20$	0.81	$0.62 \pm 0.01$
B1821+05	0.7529	318	1	$230 \pm 100$	0.64	$0.49 \pm 0.12$
		318	2	$320 \pm 090$	0.89	$1.23 \pm 0.11$
		318	3	$440 \pm 080$	1.23	$0.72 \pm 0.08$
B1857–26	0.6122	318	1	$160 \pm 50$	0.55	$0.72 \pm 0.12$
		318	2	$350 \pm 30$	1.20	$0.81 \pm 0.04$
		318	3	$480 \pm 80$	1.65	$0.88 \pm 0.08$
B2045–16	1.9617	328	1	$1000 \pm 130$	1.06	$0.31 \pm 0.030$
		328	2	$1790 \pm 040$	1.91	$0.35 \pm 0.005$
B2111+46	1.0147	333	1	$800 \pm 190$	1.66	$0.28 \pm 0.04$
		333	2	$1230 \pm 50$	2.54	$0.41 \pm 0.01$

<sup>a</sup>Cone numbering is the same as in GG2001 and GG2003 (ie. from the innermost cone outwards).

<sup>b</sup>Probably high-altitude “core”, see Section 4.2.

Note. — Errors of  $\theta'_{\text{fp}}$  are substantially underestimated, because they do not include uncertainty in  $\alpha$  and  $\beta$ .

Table 2. Surface colatitudes  $\theta'_{\text{fp}}$  of magnetic field lines associated with the lowest intensity level, derived with the method of BCW91.

Pulsar	$\nu$ [GHz]	$\theta'_{\text{fp}}$	$\pm 1\sigma$ error box	LOC <sup>a</sup> [ $\sigma$ ]
B0301+19	0.43	1.97	1.38 – 2.64	1.7
	1.42	3.03	1.97 – 4.65	2.1
B0525+21	0.43	2.28	1.70 – 3.16	2.6
	1.42	1.82	1.29 – 2.89	1.8
B1913+16	0.43	1.13	0.77 – 1.44	0.4
	1.42	0.91	0.69 – 1.12	0.4
B1914+13	1.42	0.71	< 0.80	2.3

<sup>a</sup>Level of consistency of  $\theta'_{\text{fp}}$  with 1, in units of the standard deviation  $\sigma$  derived from errors of  $r_{\text{delay}}$  and  $r_{\text{geo}}$  from table 3 in Blaskiewicz et al. (1991).

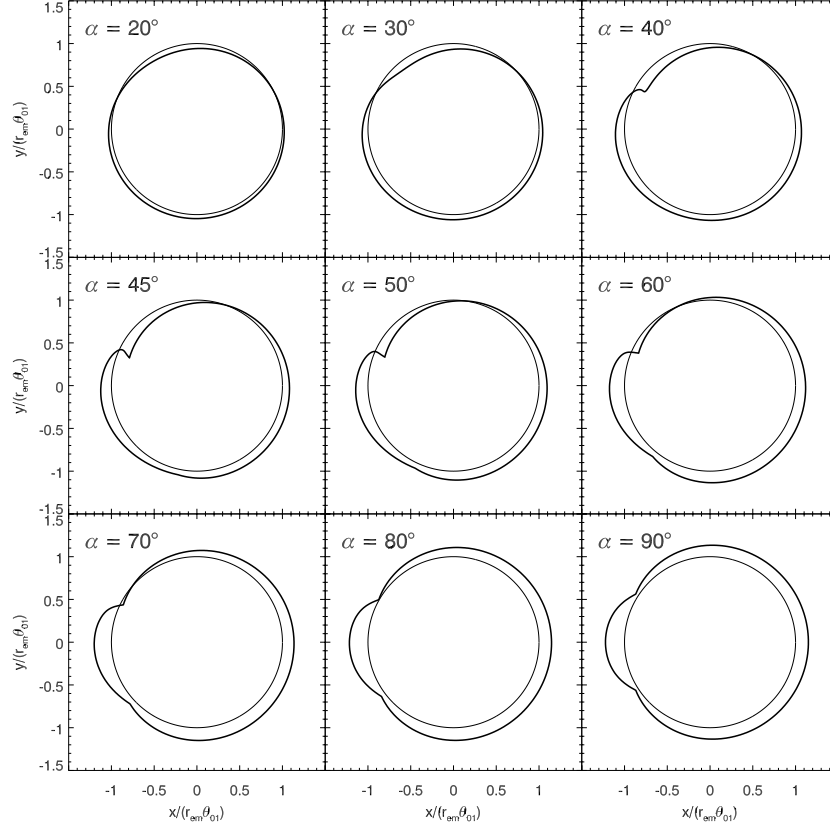


Fig. 1.— Crossection of the last open magnetic field lines with a star-centered sphere of radius  $0.01R_{lc}$  calculated for the rotating vacuum dipole (thick solid contours). This shape is identified with the shape of the outer edge of pulsar radio beam at radial distance  $r_{em} = 0.01R_{lc}$ . Different panels correspond to different dipole inclinations  $\alpha$ . In each panel, a circle of angular radius  $\theta_{01} = (r_{em}/R_{lc})^{1/2} \simeq 5.7^\circ$  is added for a reference. Note the asymmetry of the beam shape with respect to the  $x = 0$  axis and the notch present for  $\alpha \sim 40^\circ - 50^\circ$ . The magnitude of the asymmetric distortions reaches  $0.2\theta_{01} \sim 1^\circ$ , ie. it is comparable to the effects of aberration and retardation. Rotation is to the left, and the nearest rotational pole is up.